Aalborg Universitet

AALBORG UNIVERSITY
DENMARK

Droop-Controlled Inverters with Seamless Transition between Islanding and Grid-Connected Operations

Hu, Shang-Hung ; Kuo, Chun-Yi ; Lee, Tzung-Lin; Guerrero, Josep M.

Droop-Controlled Inverters with Seamless Transition between Islanding and Grid-Connected Operations

Shang-Hung Hu Chun-Yi Kuo Tzung-Lin Lee

Department of Electrical Engineering
National Sun Yat-sen University
TAIWAN
Email: tllee@mail.ee.nsysu.edu.tw

Josep M. Guerrero

Dept. Energy Technology
Aalborg University
DENMARK
Email: joz@et.aau.dk

Abstract—**This paper presents a seamless transition method for droop-controlled inverters to operate in both islanding and grid-connected modes. A local PLL and a virtual inductance are designed to ride through transient when the inverter switches between two modes with no synchronization. The proposed method can cooperatively work with well-developed droop controls so that the inverters are able to share load among them as well as subsist under transient events of the utility. Theoretical analysis and experimental results validate effectiveness of the proposed method.**

I. INTRODUCTION

Inverter-based distributed power generation systems (DPGSs) have received much attention recently due to flexible power-controlling capability. Usually, the inverter with the grid-following control is used to accomplish power conversion between the grid and DPGSs. However, this method may suffer from voltage stability, frequency variation, voltage harmonics, and cannot work in the islanding situation. Instead of the grid-following control, the grid-forming inverter is preferred because it is able to provide many ancillary services defined in IEEE Std. 1547[1], such as load regulation, reactive power compensation, and power quality improvement.

In order to integrate various DPGSs into the utility, Microgrid[2] concept was presented to assure the system with high quality and high reliability in both grid-connected and islanding operations. In the islanding mode, frequency- and voltage-droop controls are realized among inverters to share real power and reactive power in a decentralized fashion [3,4]. When going into the grid-connected mode, the inverter is controlled as a current source instead. Obviously, a coordinating system is definitely required to accomplish proper transition without undergoing transient current. Droop-controlled inverter has been presented to operate in both grid-connected and islanding modes. Acceptable steady-state performance can be accomplished, such as load sharing and voltage regulation. In case of mode transition, however, the inverter may undergo severe current transient, which might be large enough to trigger protection of the inverter due to low line impedance.
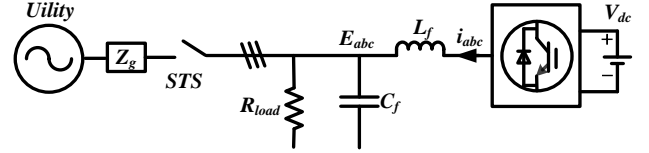

Figure 1. Circuit of the inverter connected to local load.

Virtual inductance concept was proposed to limit inrush current for plug-in of the inverter [4]. However, transient current is still significant when the upcoming inverter is out of phase with the grid.

This paper presents a seamless transition method for droop-controlled inverters. Zero-current control is proposed to suppress transient current due to asynchronous paralleling. Simultaneously, a local phase-locked-loop (PLL) is designed to obtain the angle of the inverter output voltage for correcting the angle of voltage command in the droop control. After that, the virtual inductance is realized to suppress inrush current coming from drooping operation of the inverter. Based on this algorithm, transient current between the inverter and the grid could be avoided even with no phase-synchronization used. The method could be further extended for inverter-based DPGSs to ride through power-quality events, such as voltage sag and swell.

II. OPERATION PRINCIPLES

Fig. 1 shows a droop-controlled voltage source inverter intended to supply power to the local load as well as the utility. Circuit parameters are given in TABLE I. In this paper, a seamless transition method for riding through transient is proposed to allow inverters switching between the islanding and the grid-connected modes with no requirement of grid information. The state-of-the-art droop control will be presented first, followed by the riding-through algorithm.

A. Droop control

The overall control of the inverter is shown in Fig. 2. When both SW_1 and SW_2 are at position 1, the inverter is operated in the droop-controlled mode.
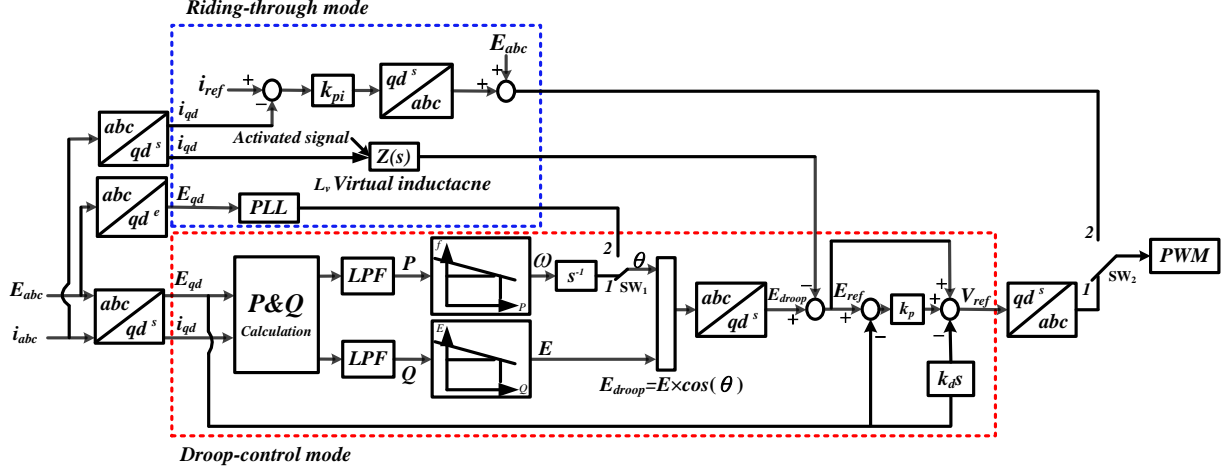
Figure 2. The proposed control block diagram.

TABLE I. CIRCUIT PARAMETERS.

Local Load	R_{load}	50	ohm
Filter Inductor	L_f	5	mH
Filter Capacitance	C_f	20	μF
Line Transmission impedance	Z_g	0.2 +j1.885	ohm

Figure 3. Flow chart of the proposed control strategy.

The voltage command is determined according to both frequency-real power and voltage-reactive power droops. Droop equations and their definitions are given in (1). Thus, various inverters are able to share workloads if their droop coefficients are chosen in inverse proportion to their rated capacities, as given in (2).

$$\omega = \omega_o - m \cdot (P_o - P); \quad E = E_o - n \cdot (Q_o - Q) \quad (1)$$

$$\begin{aligned} -m_1 P_{o1} = -m_2 P_{o2} = -m_3 P_{o3} \dots \\ -n_1 Q_{o1} = -n_2 Q_{o2} = -n_3 Q_{o3} \dots \end{aligned} \quad (2)$$

Where the ω_o is the nominal frequency, P_o is the output rated real power, E_o is the nominal voltage, Q_o is the rated output reactive power, m is the P-f droop coefficient and n is the Q-v droop coefficient.

Based on the voltage command, a proportional control plus the feedforward of the voltage command is realized to regulate output voltage in the stationary reference frame [5]. Due to the feedforward, inverter voltage can be controlled with acceptable steady-state and transient behavior. In addition, the differentiating of capacitor voltage is fed back in order to reduce the resonance on the filter capacitor C_f. As can be seen, a proportional gain K_d can be designed to accomplish a critical damped response for the voltage control loop of the inverter. Finally, PWM is realized to produce switching signals of the inverter.

B. Riding-through algorithm

In order to maintain proper operation of the inverter, we present a seamless transition method to help the inverter ride
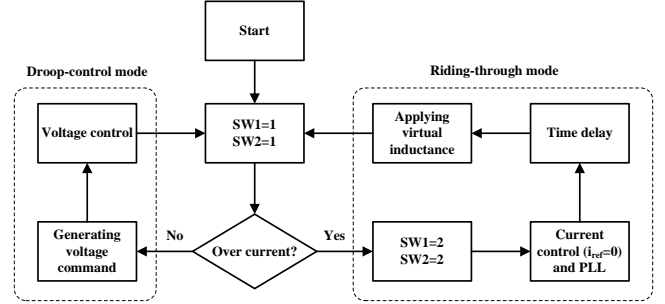
through large transient current due to asynchronous grid connection. Fig.2 shows the proposed control method, including phase-lock loop (PLL), current control, and virtual inductance. The riding-through control will be triggered when the inverter current exceeds presetting limitation. Fig.3 shows the flow chart to illustrate detailed operation. If the transient current is large enough at the closing of the STS, the inverter control will temporarily switch to the riding-through mode (SW_1 and SW_2 are at position 2). During this period, the inverter will operate at the current control mode with zero current command and the PLL will replace the angle command in the droop controller. This can correct angle difference between the inverter and the utility due to asynchronous connection. A short time delay is then required for PLL to reach the steady state. After that, a virtual inductance defined in (3) will start in operation,

$$L_v = L_{vf} - (L_{vi} - L_{vf}) \cdot e^{-t/\tau} \quad (3)$$

$$V_{Lqds} = L_v \frac{di_{qds}}{dt} \quad (4)$$

where L_{vf} and L_{vi} are final and initial inductances, respectively, and τ represents time constant. Thus, a reacted voltage in (4) is produced to reduce transient current due to angle variation of the droop control. The stability of the inverter can also be improved by the virtual inductance. After this short transient, the inverter will transfer back to the droop-controlled mode (SW_1 and SW_2 are at position 1).
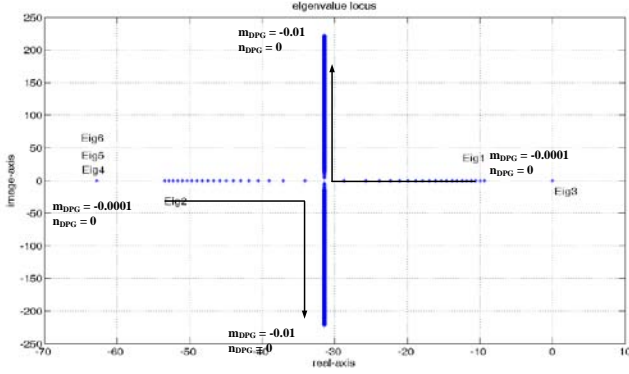
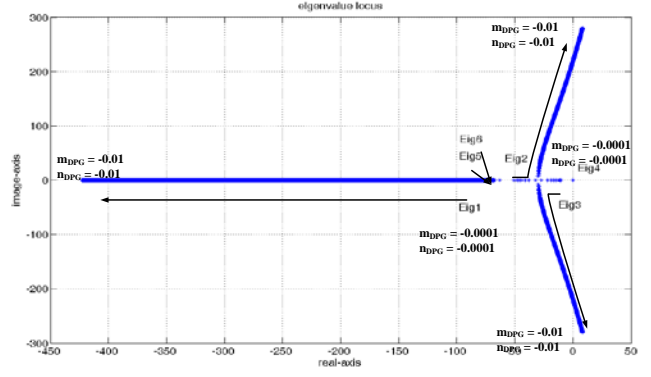Figure 4. Root locus of the inverter P-f coefficient changes from -0.0001 to -0.1.

Figure 5. Root locus of the inverter P-f and Q-v coefficients both change from -0.0001 to -0.1
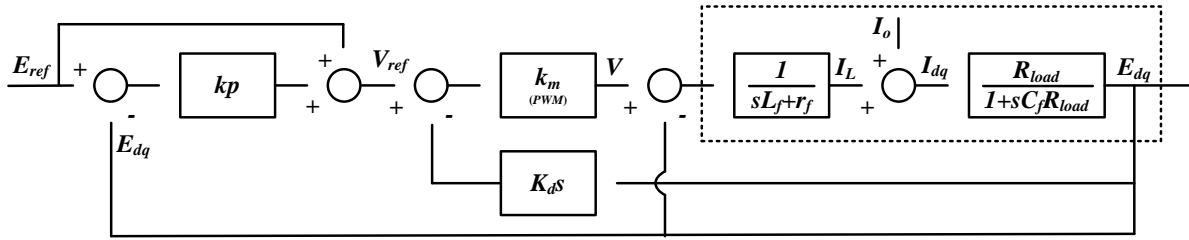

Figure 6. Multi-loop voltage control block diagram

III. DESIGN CONSIDERATIONS

A. Droop control coefficients

According to (2), the droop coefficient needs to be designed for proper load sharing. Here, we present design considerations based on the dynamic equation and root locus method. Fig.4 shows the movement of roots for varying the P-f droop coefficient m_{inv}. Note that the utility is assumed as a stiff voltage source. As can be seen, two roots become complex number when m_{inv} varies from -0.0001 to -1. Thus, this is a stable system with damping oscillation only. Next, we consider varying both n_{inv} and m_{inv}. Fig.5 shows the roots will move to the right-half of the plane with increasing both coefficients. Results show the system will become unstable for large n_{inv}. Based on the above observation, m_{inv} and n_{inv} can be chosen with an acceptable transient behavior in the stable range.

B. Multi-loop voltage control

Fig.6 shows the modeling of multi-loop voltage control, in which the dash-box represents the plant model, V_{ref} is the normalized modulation signal and E_{dq} is the output voltage of the inverter. E_{dq} to V_{ref} and E_{dq} to E_{ref} transfer functions are given in (4) and (5), respectively.

$$G(s) = \frac{E_{dq}}{V_{ref}} = \frac{k_m \frac{1}{L_f C_f}}{s^2 + \left(\frac{L_f + K_d R}{R\sqrt{L_f C_f}}\right)\cdot s + \frac{1}{L_f C_f}} = k_m G'_{LC}(s) \quad (4)$$

$$\frac{E_{dq}}{E_{ref}} = (1 + k_p)G(s) \quad (5)$$

Differential gain K_d can be designed with critically damping condition of (4) as defined in (6).

$$Q = \frac{1}{2\xi} = \frac{L_f + K_d R}{R\sqrt{L_f C_f}} : \begin{cases} > 0.5, & (under\ damping) \\ = 0.5, & (critical\ damping) \\ < 0.5, & (over\ damping) \end{cases} \quad (6)$$

As can be seen from Fig.7, the high frequency resonance may harmonics or even cause instability when $K_d = 0$. In case of $K_d = 0.00535$, the resonance is clearly suppressed and phase lagging is improved. For over-damping condition ($K_d = 0.001064$), stability is also improved, but its time response is lower than that of the critically damping case. After determining K_d, the proportional gain k_p can be obtained according to the frequency response of the voltage loop. Fig.8 shows bode plot of the open loop. Accordingly, we can choose suitable bandwidth and phase margin.

C. Virtual inductance

Fig.9 shows the simplified circuit diagram including the virtual inductance. Similarly, the dynamic equation and root locus are used for the purpose of stability analysis. Fig.10 shows the root locus when the virtual inductance L_v decreases from 5H to 80uH. As demonstrated, roots will be close to the real-axis. That means the stability of the system is improved with increasing the virtual inductance.

I. EXPERIMENTAL RESULTS

A lab-scaled prototype was developed to verify the proposed seamless transition control strategy. Test circuit is shown in Fig.11 and the parameters are given as TABLE II.
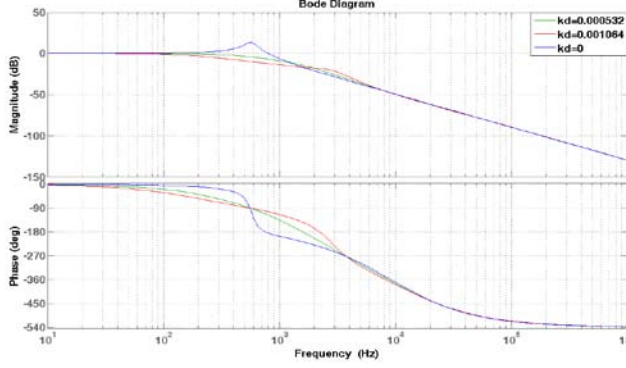
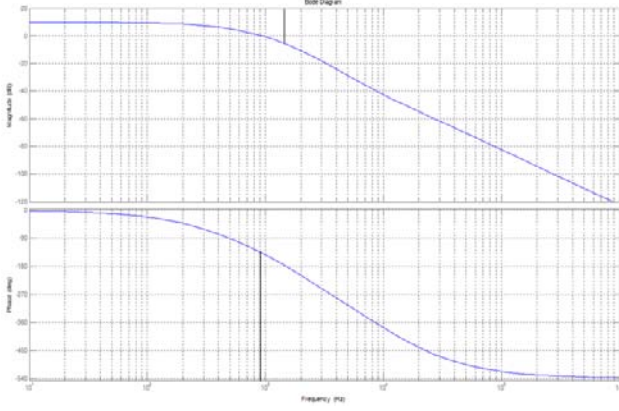Figure 7. Frequency response of three different K_d

Figure 8. Bode plot of the open loop for k_p =0.3.
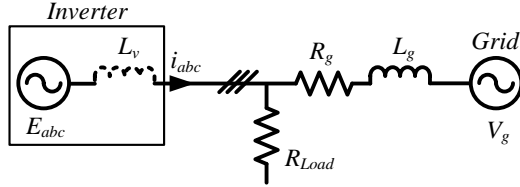(crossover frequency=762Hz, phase margin=68 °).

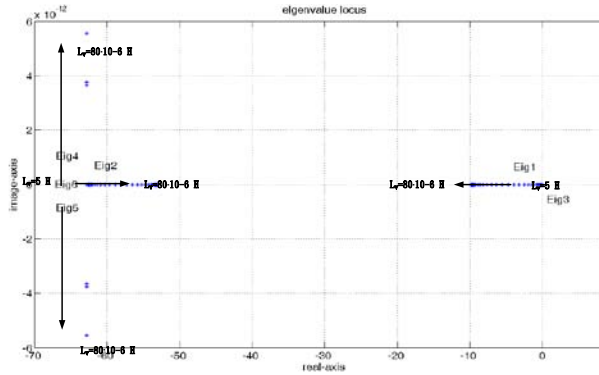Figure 9. Simplified circuit which inverter connects to grid through a virtual inductance

Figure 10. Root locus of the different virtual inductance

Nominal voltage	E_0	174.7	V
Inverter output power	P_o	1000	W
Nominal Frequency	ω_0	377	rad/s
P-ω droop	m	-0.0005	rad/J
Q-V droop	n	0	V/VAr
Filter Cut-off Frequency	ω_c	62.8	rad/s
Nominal Virtual Inductor	L_{vi}	80	μH
Initial Virtual Inductor	L_{vf}	3	H
Time Constant	τ	0.3	1/sec
Proportional gain	k_p	0.3	---
Differential coefficient	K_d	0.000532	---

Fig.12 shows the steady-state waveform when the inverter supplies a three phase load at the islanding mode, where. The inverter output a three phase balance voltage at 60Hz because of the droop controller. In order to guarantee the feasibility of the proposed seamless transition control strategy, the inverter is switched to the grid-connected operation with no grid information.

Fig.13 shows the voltages transient when the grid-connected happens at the phase difference 169.8°. At T_1, the inverter current exceeds the limitation because of the non-synchronization of the inverter and grid. At the moment, the inverter automatically switches to the riding-through mode. The current controller of the riding through mode brings the inverter output current to almost zero which is shown in Fig.14 and the PLL updates the phase angle of the voltage command at the same time. After a specific time delay, the virtual inductance is initiated at T_2 and the inverter switches back to the droop control mode. As shown, the virtual inductance can help reduce oscillating current due to the droop control. The designed virtual inductance is shown in Fig.15 with the initial value 3H and exponentially decreasing feature. Fig.16 shows transient result with no virtual inductance. Obviously, the inverter current is still high enough to trigger protection, compared with Fig.14. At the steady-state of the grid-connected operation, the inverter output rated power 1kW shows in Fig.17.

Fig.18 shows the inverter output power and the output current when the load is changed to 25Ω at T_3. At the transient, the inverter supplies the increased load. When reaching the steady state, the load is still shared by the inverter and the grid according to the designed droop control. The inverter supplies rated power 1kW and the other is from the utility. As, can be seen from Fig.19, the grid current is increased after load change.
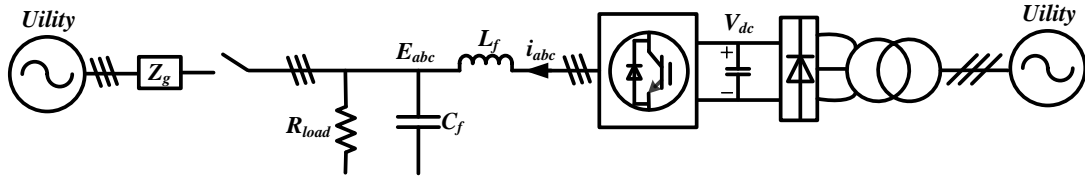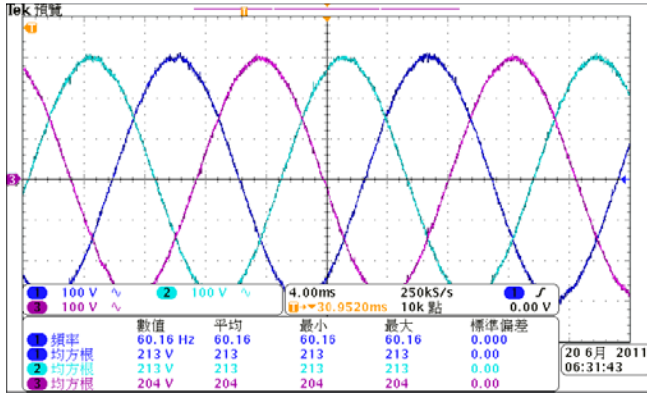
Figure 11. Experimental circuit

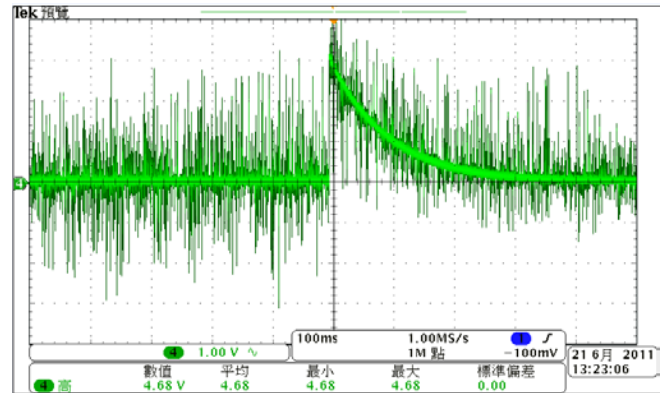Figure 12. Inverter output voltage (islanding operation)

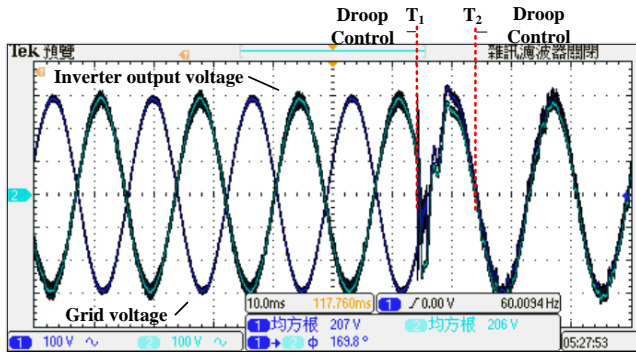Figure 15. The implement virtual inductance value (1H /1div)

Figure 13. Inverter output voltage and grid voltage (transient of inverter switching to grid-connected operation)
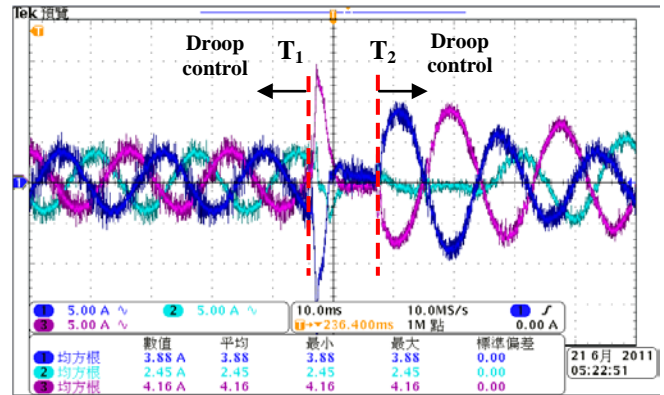

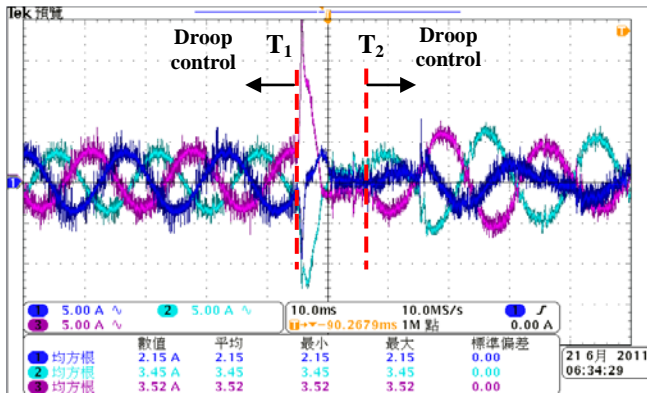Figure 16. Inverter output current without virtual inductance

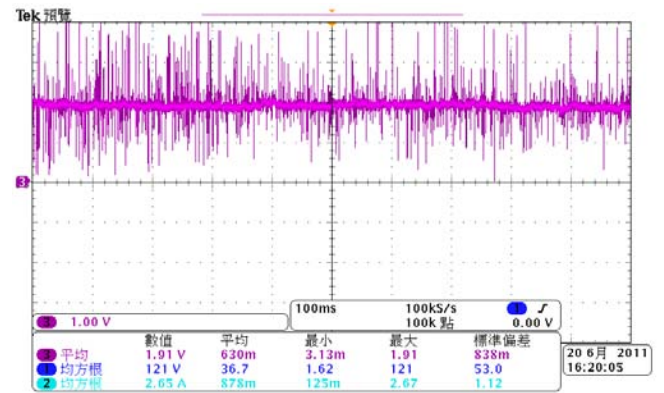Figure 14. Inverter output current with virtual inductance

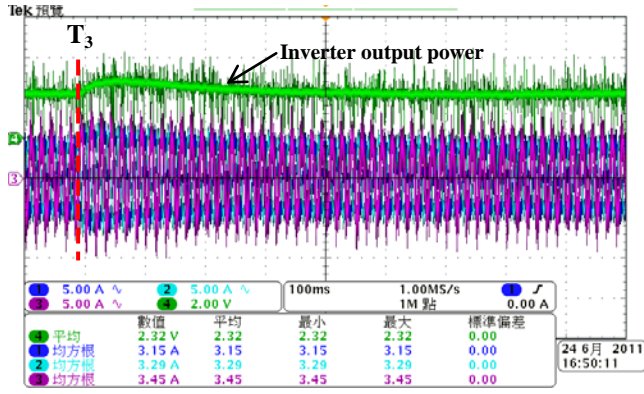Figure 17. The invert output power(500W/V)

Figure 18. The invert output power and the output current of load change (500W/V)
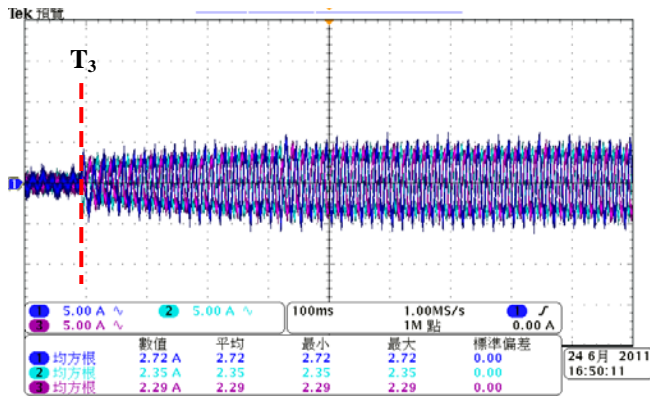

Figure 19. The grid current of load change

II. CONCLUSION

A droop-controlled inverter with seamless transition between islanding and grid-connected operations is presented. By implementing a local PLL and a virtual inductor, the inverter could ride through paralleling transient to the utility with no synchronization. This method could integrate with droop-controlled algorithms so that the inverters could share load among them as well as subsist under transient events, such as voltage sag, swell, and harmonics.

REFERENCES

[1] IEEE Standard for Interconnecting Distributed Resources with Electric Power Systems, IEEE Std 1547.2™-2008.

[2] R. Lasseter, "Microgrids," in IEEE Power Engineering Society Winter Meeting, 2002, pp. 305–308.

[3] M. C. Chandorkar and D. M. Divan, "Control of parallel connected inverters in standalone AC supply system," IEEE Trans. Ind. Applicat., vol. 29, no. 1, pp. 136–143, Jan. /Feb. 1993.

[4] J. M. Guerrero, J. C. Vasquez, J. Matas, M. Castilla, and L. G. de Vicuna, "Control strategy for flexible microgrid based on parallel line-interactive UPS systems," IEEE Trans. Ind. Electron., vol. 56, no. 3, pp. 726–736, Mar. 2009.

[5] Q. Lei, S. Yang, and F. Z. Peng, "Multi-loop control algorithms for seamless transition of grid-connected inverter", in IEEE 25th Applied Power Electronics Conference and Exposition, 2010.